© S. Hirzel Verlag
Stuttgart
ACUSTICA
Vol. 78 (1993)

Excitation of Gas Bubbles for Free Oscillations by Changing the Ambient Pressure

K. Vokurka
Department of Physics, Faculty of Electrical Engineering, Czech Technical University, Prague, Czechoslovakia

Excitation of Gas Bubbles for Free Oscillations by Changing the Ambient Pressure

Summary

Experimental data given in the literature on free oscillations of gas bubbles excited by changing the ambient pressure in a liquid are analyzed. It is found that this excitation technique is rather effective in that it enables a broad range of oscillation intensities to be obtained. The highest oscillation intensities are obtained when the duration of the driving pressure pulse is comparable with the compression time of the bubble. As with other excitation techniques, higher damping of bubble oscillations than predicted by theory is observed.

Anregung von Gasblasen zu freien Schwingungen durch Änderung des Umgebungsdrucks

Zusammenfassung

Es werden die experimentellen Literaturdaten über freie Schwingungen von Gasblasen analysiert, die durch Änderung des Umgebungsdrucks angeregt werden. Es zeigt sich, daß diese Art der Anregung insofern ziemlich effektiv ist, als sie einen breiten Bereich von Schwingungsintensitäten zuläßt. Die höchsten Schwingungsintensitäten wurden erhalten, wenn die Dauer des erregenden Druckimpulses vergleichbar mit der Kompressionszeit der Blase ist. Wie auch bei anderen Anregungsmethoden, werden höhere Dämpfungen der Blasenschwingungen beobachtet als die von der Theorie vorhergesagten.

Excitation de bulles de gaz pour oscillations libres par changement de pression ambiante

Sommaire

On a procédé à une analyse des résultats expérimentaux que l'on trouve dans la littérature spécialisée sur les oscillations libres de bulles de gaz engendrées par changement de la pression ambiante dans un liquide. Il apparaît que cette technique d'excitation est relativement efficace puisqu'elle permet d'obtenir une forte dynamique de l'intensité des oscillations. Les intensités d'oscillation les plus élevées s'obtiennent lorsque la durée de l'impulsion de pression d'excitation est comparable à la durée de compression de la bulle. En ce qui concerne les autres techniques d'excitation, on a observé un amortissement des oscillations des bulles supérieur à ce que prévoit la théorie.

1. Introduction

Bubbles oscillating in liquids may both perform useful work, as in ultrasonic cleaners, and act harmfully, as for example cavitation in hydraulic machinery. For both these reasons oscillating bubbles have been a subject of intensive research for a long time. Recent work concentrates on low-energy free oscillations in response to a short-lived excitation [1, 2], low-energy stable oscillations in a periodic driving field [3], high-energy oscillations in response to periodic driving fields [4], acoustic diagnostic pulses [5], acoustic lithotriptic pulses [6], step changes in pressure [7], laser-irradiation [8–10], or electrical discharges [11]. Further studies deal with dynamics of periodically driven bubble clouds [12], and passive emissions from collective oscillations of bubble clouds [13–15]. Finally, the contribution of changes in ambient pressure to the excitation of passive acoustic emissions from oceanic bubbles [16–18], the thermal behaviour of bubbles [19], and shape-resonant mechanism and associated exchange of energy between the shape oscillations and the breathing mode [20, 21], are also current topics of great interest.

Excitation of gas bubbles for free oscillations by changing the ambient pressure in a liquid is one of the basic excitation techniques [22]. This technique was used in experimental studies on bubble dynamics, for example, by Smulders and van Leeuwen [23], Jensen [24], Shima et al. [25] and Vokurka et al. [7].

In this paper, the experimental data given in Refs. [23–25] will be analyzed with the aim of determining the intensities of bubble oscillations. For this purpose, a method based on scaling functions and described in Ref. [26] will be used. The results obtained are useful for comparison of the oscillation intensities of bubbles excited by different techniques and when planning new experiments on bubble dynamics. The results also confirm earlier findings [26] regarding excessive damping of oscillating bubbles.

Received 8 May 1992,
accepted 12 August 1992.

K. Vokurka, Department of Physics, Faculty of Electrical Engineering, Czech Technical University, Prague, CS-11627, present address: Švédská 27, Jablonec n. N., CS-46602, Czechoslovakia.

2. Experimental techniques

Several basic results regarding the excitation of gas bubbles for free oscillations by changing the ambient pressure in the liquid, p_∞, were given in Ref. [22]. According to that study, in order to excite the bubble, the ambient pressure must be either increased or decreased. However, to ensure that the bubble remains a pure gas bubble (the case considered here), the ambient pressure should not drop below the liquid vapour pressure, P_v. Thus, if the maximum value of the ambient pressure change is denoted as Δp, one obtains two ranges of possible values for Δp: (i) $\Delta p > 0$, (ii) $P_v - p_{\infty i} < \Delta p < 0$. Here $p_{\infty i}$ is the initial value of the ambient pressure.

With regard to the time interval, ΔT, during which the new ambient pressure occurs (the rise time of the pressure change Δp will be denoted as Δt), two cases can be distinguished. In the first case it is assumed that the new ambient pressure $p'_\infty = p_{\infty i} + \Delta p$ is relatively constant and lasts for a longer time than the interval during which the bubble is being observed. This situation was symbolically denoted in Ref. [22] as $\Delta T \to \infty$. In the second case the ambient pressure p_∞ changes significantly during the interval in which the bubble is being observed. This situation was denoted in Ref. [22] as $\Delta T < \infty$, and the pressure change was referred to as "transient".

There are basically two ways to change the ambient pressure in a liquid containing a gas bubble. First, the liquid with the gas bubble is at "rest" and a pressure disturbance (a wave of compression, a wave of rarefaction, or a combination of both) travels through the liquid. Second, the liquid with the bubble flows through a region where the pressure is either increased or decreased.

Of these possibilities, only the method based on the wave of compression (usually a shock wave) was used experimentally. To generate a relatively long-lasting ambient pressure increase ($\Delta p > 0$, $\Delta T \to \infty$), Smulders and van Leeuwen [23] and Vokurka et al. [7] used a shock tube. On the other hand, Jensen [24], and Shima et al. [25] produced a transient ambient pressure change ($\Delta p > 0$, $\Delta T < \infty$) by underwater explosions and by spark discharges, respectively.

If only these experiments are considered, a better designation of the excitation technique would probably be "excitation by pressure pulses". However, the designation "excitation by changing the ambient pressure" indicates that there is a broader spectrum of possible excitation techniques (as discussed above), even if they have not as yet been used experimentally.

The case when $\Delta p \leqq P_v - p_{\infty i}$ has been deliberately omitted from this discussion. This is because generation and excitation of bubbles under such circumstances is known as cavitation, and cavitation bubbles, with respect to their importance, were discussed separately [27].

3. Evaluation of experimental data

3.1. Experiment of Smulders and van Leeuwen

In the experiment of Smulders and van Leeuwen [23] a shock tube was employed to generate an ambient pressure change (pressure step wave) in water. This pressure step excited a gas bubble, floating upward in the liquid, for free oscillations. According to the authors, the rise time of the pressure step, Δt, was less than 4 μs and the pressure behind the front was almost constant for approximately $\Delta T = 3$ ms. As the bubble observations lasted only 550 μs, it is evidently the case that $\Delta T \to \infty$.

Let us evaluate the data given in Fig. 7 of Ref. [23]. In this particular case the initial radius of the bubble was $R_i = 1$ mm, the initial ambient pressure $p_{\infty i} = 50$ kPa, and the increased pressure behind the step wave front $p'_\infty = 180$ kPa. As the gas inside the bubble was air, and is here assumed to behave adiabatically, the polytropic exponent takes a value equal to γ, the ratio of the specific heats of the gas, which for air equals 1.4. From the values of the pressure given above, it follows that the non-dimensional pressure step strength was

$$\Delta p^* = \Delta p / p_{\infty i} = (p'_\infty - p_{\infty i})/p_{\infty i} = 2.6$$

and the non-dimensional pressure at the bubble wall at the beginning of the compression was

$$p_{\infty i}/p'_\infty = 0.28\,.$$

Then the corresponding amplitude of the first bubble oscillation $A_1 = R_i/R'_e$ (here R'_e is the bubble "equilibrium" radius under a new ambient pressure p'_∞; see also the Appendix B for the definition of the amplitude A) can be determined by means of the formula [7]

$$A_1 = (p_{\infty i}/p'_\infty)^{-1/3\gamma}. \tag{1}$$

Eq. (1) was derived under the assumption that the pressure increase from $p_{\infty i}$ to p'_∞ was accomplished in a much shorter time than the time of the first bubble compression, T_{c1} (T_{c1} is defined as a time, during which the bubble is compressed from the initial radius R_i to the first minimum radius R_{m1}). As the rise time of the pressure was $\Delta t \approx 4$ μs and $T_{c1} \approx 94$ μs, it can be seen that this assumption is fulfilled here. After substituting into eq. (1), it will be found that the first amplitude is $A_1 = 1.35$.

The non-dimensional first minimum bubble radius as estimated from Fig. 7 of Ref. [23] is $Z_{m1} = R_{m1}/R_i = 0.53$ (here the initial radius R_i was taken at

$t = 1$ μs and the first minimum radius R_{m1} at $t = 94$ μs). Similarly the non-dimensional second maximum radius estimated from Fig. 7 of Ref. [23] equals $Z_{M2} = R_{M2}/R_i = 0.93$ (the estimate of the second maximum radius R_{M2} represents an average taken at times $t = 178$ μs and $t = 182$ μs and from two mutually perpendicular directions). The experimental radii are compared with the theoretical data in Fig. 1 (the theoretical variations of Z_{m1} and Z_{M2} with the pressure step Δp^* shown in Fig. 1 were calculated using the model given in the Appendix A). It can be seen from Fig. 1 that the experimental minimum radius Z_{m1} agrees rather well with the theoretical data. As far as the experimental maximum radius Z_{M2} is concerned, it is smaller than the theoretical value. A smaller Z_{M2} usually indicates a larger dissipation of the bubble energy than considered by the theoretical model (see, e.g. the Appendix B for the definition of a damping factor α_2, which equals Z_{M2}). However, the results reported in paper [7] indicate that the processes involved in this particular excitation technique are rather complex and at present no satisfactory answer can be given to explain why the maximum radius Z_{M2} is so small. No error bars are shown in Fig. 1 since the procedure used to determine Z_{m1} and Z_{M2} has a high accuracy.

3.2. Experiment of Jensen

To measure the pressure inside a gas bubble directly, Jensen [24] developed an experimental arrangement where the bubble was enclosed in a thin rubber membrane. The excitation of the bubble for free oscillations was brought about by means of a shock wave generated by a small electric detonator. The distance of the bubble centre from the detonator, d, varied from 0.3 to 1.5 m. Hence, according to eq. (3) in Ref. [24] the shock wave pressure Δp at the place of the bubble ranged from 2.3 to 14.1 MPa. The main part of the shock wave was concentrated within the first 50 μs after the shock front (i.e. $\Delta T \approx 50$ μs), which is a much shorter interval than the time of the first bubble compression T_{c1}. (A typical value of T_{c1} is 0.6 ms – see Table III). Hence the ambient pressure change was a transient one ($\Delta T < \infty$). The hydrostatic pressure at the place of the bubble was approximately $p_{\infty i} = 100$ kPa, because Jensen used an open experimental water channel of dimensions $0.6 \times 0.7 \times 7$ m exposed to atmospheric pressure.

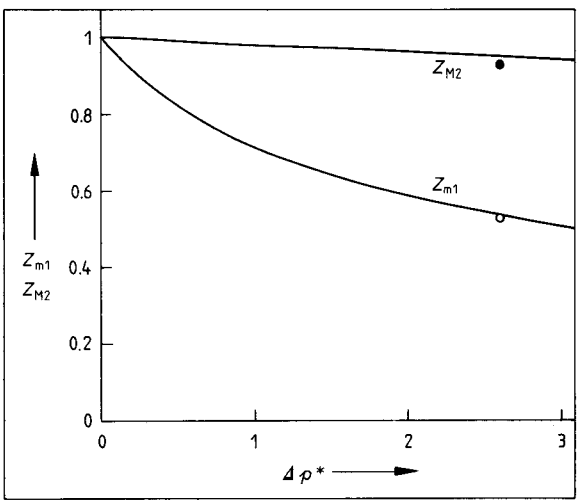

Fig. 1. Variation of the first minimum radius Z_{m1} and second maximum radius Z_{M2} with the pressure step strength Δp^* (—— theory, o and • experiment).

In the experiments the initial bubble radii R_i ranged from 5 to 15 mm. With respect to the attained bubble oscillation amplitudes (to be determined later), it can be seen in the bubble map [26] that these bubbles belong to the so-called scaling bubbles, for which heat losses should be insignificant. This was also experimentally verified by Jensen [24], who found that the absolute pressure at the bubble wall, P, is related to the bubble radius, R, by the adiabatic law, i.e.

$$P = p_{\infty i}(R/R_i)^{-3\gamma}. \tag{2}$$

As the gas inside the bubble was air, the adiabatic exponent is $\gamma = 1.4$.

An example of the computed time histories of the bubble radius, R, and pressure at the bubble wall, P, is given in Figs. 2 and 3, respectively. Displayed time histories were computed with Herring's simplified equation of motion for the bubble wall as given in Appendix A. The transient change of the ambient pressure was assumed to have the simple form of an exponential pulse, given also in Appendix A. The pressure pulse parameters Δp and ϑ (ϑ is the time constant of the exponential pulse) were selected in such a way as to give a bubble response similar to the experimental one as given in Fig. 6 or Ref. [24] and discussed later in this section. However, no special efforts were made to obtain complete similarity. Note that the driving pressure pulse p_∞ shown schematically in Fig. 2 represents a sharp spike in comparison with a relatively slow bubble response.

Some basic quantities used in the following paragraphs when evaluating experimental data are also given in Figs. 2 and 3. For example, P_M and P_m are the absolute maximum and minimum pressures at the bubble wall, and P_p and P_t represent the acoustic peak and trough pressures at the bubble wall, respectively. The mutual relations among these pressures are as follows:

$$P_M = P_p + p_{\infty i}, \tag{3}$$

$$P_m = P_t + p_{\infty i}. \tag{4}$$

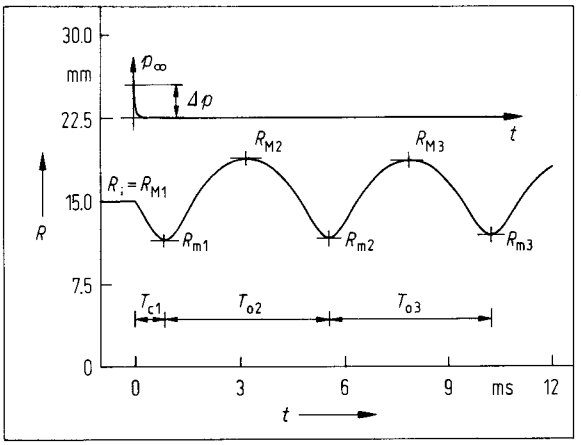

Fig. 2. Computed time history of the bubble wall motion.

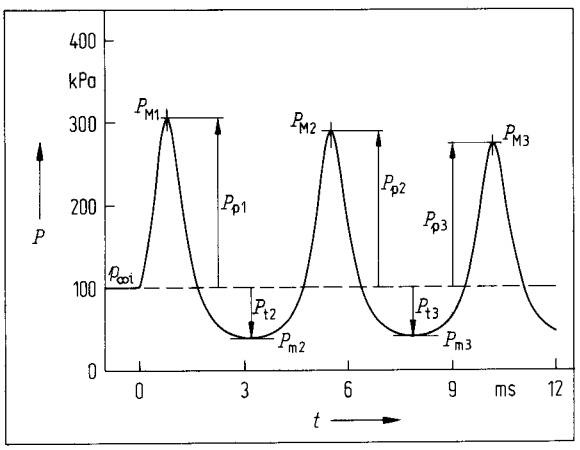

Fig. 3. Computed time history of the pressure at the bubble wall.

Let us now evaluate the experimental data given in Ref. [24]. First, from Fig. 8 of Ref. [24] it follows that in the experiments the first peak pressure at the bubble wall, P_{p1}, ranged from 10 kPa to 2.5 MPa. Using eqs. (2) and (3) it can be determined that the non-dimensional first minimum bubble radii $Z_{m1} = R_{m1}/R_i$ ranged from 0.978 to 0.461. Using the scaling function $Z_m(A)$ given in Fig. 4 (this function was calculated using the model given in Appendix B) it can be found that the first amplitudes of bubble oscillations A_1 thus ranged from 1.01 to 1.41. These values of A_1 can be used in conjunction with the bubble sizes to locate the bubbles in the bubble map [26] (as was done earlier).

As a second example, the pressure variations inside the oscillating bubble as given in Fig. 6 of Ref. [24] will be considered. In this particular case, the initial bubble radius was $R_i = 15$ mm and the distance from the charge was $d = 0.5$ m. The shock pressure (as determined from eq. (3) of Ref. [24]) was $\Delta p = 7.92$ MPa and the first peak pressure at the bubble wall (as determined from Fig. 8 of Ref. [24]) was $P_{p1} = 230$ kPa. The values of subsequent peak and trough pressures were estimated directly from Fig. 6 of Ref. [24] by comparison with P_{p1}. These peak and trough pressures and the corresponding maximum and minimum pressures are given in Table I. It should be noted here that since no calibrated vertical scale is given in Fig. 6 of Ref. [24], these estimates are necessarily rather poor.

From the pressures given in Table I it is now possible to determine, using eq. (2), the minimum and maximum radii R_{m1}, R_{M2}, R_{m2}, R_{M3}, and R_{m3}, and thus also the non-dimensional minimum radii $Z_{m1} = R_{m1}/R_i$, $Z_{m2} = R_{m2}/R_{M2}$, $Z_{m3} = R_{m3}/R_{M3}$, and the second damping factor $\alpha_2 = R_{M3}/R_{M2}$ (for a definition of the radii see Fig. 2). These quantities, together with the estimated amplitudes of bubble oscillation (as determined from the scaling functions $Z_m(A)$ and $\alpha(A)$ given in Fig. 4) are summarized in Table II.

Table I. Peak, trough, and corresponding maximum and minimum pressures at the bubble wall.

$P_{p1} = 230$ kPa	$P_{M1} = 330$ kPa
$P_{t2} = -54$ kPa	$P_{m2} = 46$ kPa
$P_{p2} = 205$ kPa	$P_{M2} = 305$ kPa
$P_{t3} = -46$ kPa	$P_{m3} = 54$ kPa
$P_{p3} = 80$ kPa	$P_{M3} = 180$ kPa

Table II. Minimum radii, second damping factor, and corresponding amplitudes of the oscillating bubble (the amplitudes being determined from the scaling functions $Z_m(A)$ and $\alpha(A)$).

$Z_{m1} = 0.75$	$A_1 = 1.15$
$Z_{m2} = 0.64$	$A_2 = 1.24$
$Z_{m3} = 0.75$	$A_3 = 1.15$
$\alpha_2 = 0.96$	$A_2 = 1.92$

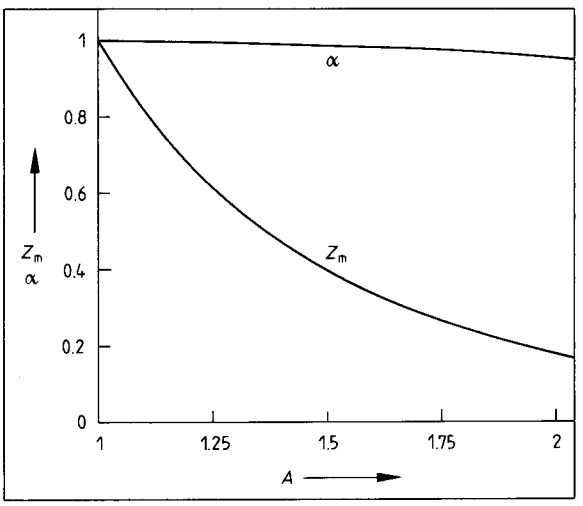

Fig. 4. Scaling functions $Z_m(A)$ and $\alpha(A)$.

Note that in the case of a transient pressure change, strictly speaking, the amplitude cannot be defined in the usual way as the ratio of the maximum and equilibrium radii. The reason for this is that the equilibrium radius has lost its usual meaning for a variable ambient pressure. (Similarly, the damping factor can be defined in its usual sense only for environments with a relatively constant ambient pressure.) Nevertheless the amplitude still falls within the definition of an oscillation intensity measure and as such can be determined via the scaling functions of some measurable quantities. This approach has been adopted in the present and in the following sections.

As follows from Table II, the amplitude of the second oscillation, as determined from Z_{m2}, is $A_2 = 1.24$. A theoretical damping factor corresponding to this amplitude can be determined as above from the function $\alpha(A)$ given in Fig. 4, and it follows that $\alpha_2 = 0.99$. However, the experimental damping factor in Table II was determined directly as the ratio of R_{M3} and R_{M2}, and its was found that $\alpha_2 = 0.96$. From the scaling function given in Fig. 4 it then follows that the amplitude corresponding to this value of α_2 is $A_2 = 1.92$. Thus, two pairs of different values of A_2 and α_2 are obtained. A possible interpretation of these inconsistencies will be given in Section 4.

Let us also determine the "average" ambient pressures $\langle p_\infty \rangle$ during each phase of the bubble oscillations. These "average" values can be found from the relation

$$\langle p_\infty \rangle = \varrho_\infty (T_{zc} R_M / T_c)^2, \tag{5}$$

which follows from a definition of the non-dimensional time of the bubble compression T_{zc}. In eq. (5), $\varrho_\infty = 1000\ \mathrm{kg/m^3}$ is the density of the water. For the amplitudes given in Table II the corresponding values of T_{zc} can be determined from Fig. 5 (the scaling function $T_{zc}(A)$ displayed in Fig. 5 was obtained using the model given in the Appendix B). The maximum radii R_M were computed from data given in Table I using eq. (2). Finally the times of compression T_{c1}, $T_{c2} = T_{o2}/2$, and $T_{c3} = T_{o3}/2$ were estimated from Fig. 6 of Ref. [24] (here T_{o2} and T_{o3} are the times of the second and third oscillations, respectively, see Fig. 2). The times of the bubble compression and corresponding "average" ambient pressures as computed from eq. (5) are given in Table III. As can be seen from Table III, the "average" ambient pressures do not drop below the initial ambient pressure $p_{\infty i}$. This indicates a complex wave field in the test channel (probably due to wave reflections) because normally the shock wave from an underwater explosion should be followed by a wave of rarefraction [28]. Unfortunately, Jensen [24] does not report the time development of the pressure p_∞ so that comparison of the estimates obtained here with measured values cannot be undertaken.

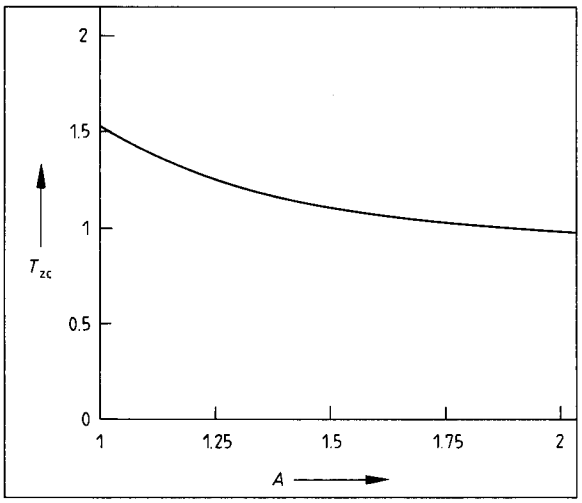

Fig. 5. Scaling function $T_{zc}(A)$.

Table III. Times of bubble compression and corresponding values of the "average" ambient pressure.

$T_{c1} = 0.6$ ms	$\langle p_{\infty 1} \rangle = 1.14$ MPa
$T_{c2} = 1.9$ ms	$\langle p_{\infty 2} \rangle = 145$ kPa
$T_{c3} = 2.25$ ms	$\langle p_{\infty 3} \rangle = 109$ kPa

3.3. Experiment of Shima et al.

Shima et al. [25] used an air bubble ($\gamma = 1.4$) of an initial radius $R_i = 1$ mm which was impinged on by a shock wave generated at the instant of a spark discharge in water. The shock wave strength at the place of the gas bubble was approximately $\Delta p = 5$ MPa (the air bubble was situated at a distance $d \approx 5$ mm from the discharge centre), and the positive part of the shock wave lasted approximately for $\Delta T = 10$ μs (the value of ΔT can be estimated from Fig. 3 of Ref. [29]).

Shima et al. [25] measured a peak pressure in the bubble pulse, p_{p1}, that was radiated by the air bubble at its first compression. From Fig. 5 in Ref. [25], for example, it follows that at a distance from the air bubble centre $r = 6$ mm, the peak pressure at the bubble pulse was $p_{p1} = 2$ MPa. The initial ambient pressure in the liquid was $p_{\infty i} = 100$ kPa. Finally, the time of the first bubble compression can be estimated from Fig. 2 in Ref. [25] as being approximately $T_{c1} \approx 25$ μs.

From these values the non-dimensional first peak pressure in the bubble pulse is $p_{zp1} = (p_{p1}/p_{\infty i}) r/R_i = 120$. Then, using the scaling function $p_{zp}(A)$ given in Fig. 6 and computed with the model given in the Appendix B, it can be determined that the corresponding amplitude of the first oscillation is $A_1 = 3.3$.

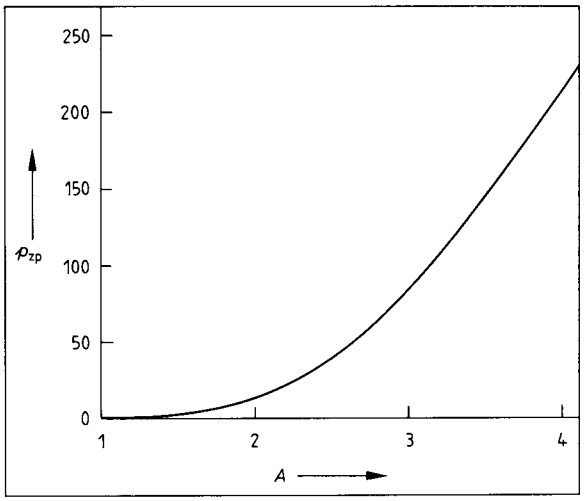

Fig. 6. Scaling function $p_{zp}(A)$.

4. Discussion

Excitation of gas bubbles for free oscillations by changing the ambient pressure is a very effective method which makes it possible to excite the bubbles to oscillate with a broad range of amplitudes (in the examples studied here A_1 ranged from 1.01 to 3.3). As shown theoretically in Ref. [22], this excitation technique is very sensitive to the length, ΔT, of the driving pressure pulse. The maximum amplitudes are obtained for a given pulse strength Δp and for a square waveform if $\Delta T/T_{c1} = 1$. This is in good agreement with the experimental data analyzed in this paper. For example, as discussed above, Jensen [24] used a driving shock wave having values $\Delta p = 7.92$ MPa and $\Delta T = 50$ μs. The corresponding amplitude of the bubble oscillation was $A_1 = 1.15$ and the compression time $T_{c1} = 0.6$ ms (see Table III). On the other hand, Shima et al. [25] used a driving shock wave having values $\Delta p = 5$ MPa and $\Delta T = 10$ μs. In this experiment the bubble oscillated with a much larger amplitude $A_1 = 3.3$ and the compression time was $T_{c1} = 25$ μs.

Thus, though the pressures Δp were of the same order in these two tests, the amplitudes of bubble oscillations A_1 differed substantially. As said above, the reason for this is the mutual relation between ΔT and T_{c1}. While in the first case $\Delta T/T_{c1} = 0.083 \ll 1$, the ratio in the second case is $\Delta T/T_{c1} = 0.4$, and hence a more effective excitation ensues. (It should be noted that according to eq. (5), T_c is dependent on Δp, R_M, and to some extent also on A).

Due to sound radiation, an exact scaling is not possible between bubbles oscillating at different ambient pressures. Hence the bubble wall motion will be different for each form and value (Δp) of the ambient pressure change. It follows then that the bubble map [26], which was determined for a constant ambient pressure $p_\infty = 100$ kPa, should be used only with reservation for other pressures. Also, strictly speaking, the amplitudes should not be determined via the values of Z_m or p_{zp}, as was done in Sections 3.2 and 3.3. However, as the highest ambient pressures occurred just at the beginning of the compression phase, the errors introduced by using the scaling functions $Z_m(A)$ and $p_{zp}(A)$, computed for $p_\infty = 100$ kPa, should be small.

When analysing the data in Section 3.2, the damping factor computed from the experimental maxium radii, $\alpha_2 = 0.96$, was lower than that corresponding to the amplitude $A_2 = 1.24$ (this amplitude was determined from the minimum radius and the respective damping factor is $\alpha_2 = 0.99$). The author's experience is that the value of the minimum radius usually is in agreement with the theory (see, e.g., Fig. 1, and the discussion in Ref. [26]) and hence the value of the amplitude $A_2 = 1.24$ is considered as being quite reliable. Assuming this is true, then a damping factor lower than that pedicted by the theory indicates either an increased energy dissipation in a real bubble or, similarly, an omission of some dissipative mechanism in the theoretical model. However, this omitted damping mechanism is a little mysterious because as a consequence of the relatively large bubble size, thermal losses may be excluded. In addition, because of the rubber membrane, some other mechanisms, such as excessive gas cooling in protuberances, loss of the gas from the main bubble in the form of microbubbles, etc., also cannot be considered. Unfortunately, lack of more extensive experimental data prevents us from drawing specific conclusions regarding this dissipative mechanism at present.

In the experiments discussed a non-spherical bubble shape was occasionally observed. As recently shown by Longuet-Higgins [20, 21], in the presence of shape distortions, an exchange of energy between the shape oscillations and a breathing mode exists. However, as we concentrated on early stages of the bubble oscillation, where the departure from sphericity was usually small, we believe it was not necessary to consider this energy exchange here.

5. Conclusion

In the paper, experiments described in Refs. [23–25] were analyzed with the aim of determining the intensities of bubble oscillations. The results obtained are summarized in Table IV. As follows from Table IV, the excitation of bubbles for free oscillations by changing

Table IV. Amplitudes of oscillations and sizes of experimental bubbles.

Source work	Amplitude A	Bubble size R_i mm
[23]	1.35	1
[24]	1.01–1.41	5–15
[25]	3.3	1

the ambient pressure enables one to obtain a rather broad range of oscillation amplitudes. It was also found that the highest oscillation intensities were obtained when the duration of the driving pressure pulse was comparable with the compression time of the bubble. Finally, as with other experiments [26], an increased damping of the bubble wall motion was observed as well.

Appendix A

Though in the case of the experimental bubbles departures from sphericity can occur, the following theory assumes, for simplicity, that the bubble remains spherical at all times. As shown in Ref. [30], for moderate intensities of bubble oscillations, Herring's simplified equation for the wall motion gives the same results as more sophisticated models. This equation has the form

$$\ddot{R}R + (3/2)\dot{R}^2 = (1/\varrho_\infty)(P - p_\infty + \dot{P}R/c_\infty). \qquad (A1)$$

Here R denotes the bubble radius, ϱ_∞ the liquid density, P the pressure in the liquid at the bubble wall, p_∞ the time dependent ambient pressure, and c_∞ the speed of sound in the liquid. Dots denote differentiation with respect to time, and the initial conditions of eq. (A1) are $R(0) = R_i$ and $\dot{R}(0) = 0$.

To obtain the theoretical values of the first minimum radius, R_{m1}, and the second maximum radius, R_{M2}, given in Fig. 1, the time dependent ambient pressure was assumed in the form

$$p_\infty = \begin{cases} p_{\infty i} & t < 0, \\ -p_{\infty i} + \Delta p\, t/\Delta t & 0 \leqq t \leqq \Delta t, \\ p_{\infty i} + \Delta p = p'_\infty & \Delta t < t. \end{cases} \qquad (A2)$$

The pressure in the liquid at the bubble wall was computed using the equation:

$$P = (p_{\infty i} + 2\sigma/R_i)(R_i/R)^{3\gamma} - 2\sigma/R - 4\eta\dot{R}/R. \qquad (A3)$$

Here γ is the ratio of the specific heats for the gas inside the bubble, σ the surface tension and η the dynamic viscosity of the liquid.

When computing the radius and pressure time histories given in Figs. 2 and 3, the time dependent ambient pressure was assumed in the form

$$p_\infty = \begin{cases} p_{\infty i} & t < 0, \\ p_{\infty i} + \Delta p \exp(-t/\vartheta) & t \geqq 0. \end{cases} \qquad (A4)$$

Here ϑ is a suitable time constant. The pressure at the bubble wall was computed from eq. (2).

Data given in Figs. 1 to 3 were computed for air bubbles in water, i.e., the physical constants had values:

$\varrho_\infty = 1000\ \mathrm{kg/m^3}$, $c_\infty = 1450\ \mathrm{m/s}$, $\sigma = 0.072\ \mathrm{N/m}$,
$\eta = 10^{-3}\ \mathrm{kg\,s^{-1}\,m^{-1}}$, $\gamma = 1.4$.

In the case of Fig. 1, the rise time of the pressure step was assumed to be $\Delta t = 5\ \mu\mathrm{s}$, and the pressure step strength Δp ranged from 0 to 150 kPa. The initial bubble radius was $R_1 = 1$ mm and the initial ambient pressure $p_{\infty i} = 50$ kPa. The computed quantities are displayed in a non-dimensional form, i.e. $Z_{m1} = R_{m1}/R_i$, $Z_{M2} = R_{M2}/R_i$, and $\Delta p^* = \Delta p/p_{\infty i}$.

In the case of Figs. 2 and 3, the shock wave pressure was assumed to be $\Delta p = 5$ MPa, the time constant $\vartheta = 15\ \mu\mathrm{s}$, the initial bubble radius $R_i = 15$ mm, and the initial ambient pressure $p_{\infty i} = 100$ kPa.

Appendix B

Gilmore's equation of motion for the bubble wall, which is suitable for more intensive oscillations, has the form (see, e.g. Ref. [30] for the source works containing further details)

$$\ddot{R}R(1 - \dot{R}/C) + (3/2)\dot{R}^2(1 - \dot{R}/3C)) = H(1 + \dot{R}/C) + R\dot{H}/C(1 - \dot{R}/C). \qquad (B1)$$

The velocity of sound in the liquid at the bubble wall can be found as

$$C = c_\infty[(P + B)/(p_\infty + B)]^{(n-1)/2n}, \qquad (B2)$$

and the enthalpy difference between the liquid at pressures P and p_∞ under isentropic conditions as

$$H = (1/\varrho_\infty)\, n/(n-1)(p_\infty + B) \cdot \{[(P + B)/(p_\infty + B)]^{(n-1)/n} - 1\}. \qquad (B3)$$

In eqs. (B2) and (B3), B and n are constants in the Tait equation of state for a liquid. The initial conditions of eq. (B1) are $R(0) = R_M$ and $\dot{R}(0) = 0$, where R_M is an initial maximum radius. (In this section, numerical indices have been omitted, where possible, for simplicity.)

When computing the scaling functions given in Figs. 4 to 6, the ambient pressure p_∞ was assumed to be constant, i.e., $p_\infty = p_{\infty i}$, and the pressure at the

bubble wall was assumed in the form

$$P = P_m (R/R_M)^{-3\gamma}. \quad \text{(B4)}$$

In eq. (B4), the initial minimum pressure $P_m < p_\infty$ represents a parameter determining the intensity of the bubble oscillation. However, for the purpose of comparison with other results, it is convenient to use the amplitude A defined as [26]

$$A = R_M/R_e. \quad \text{(B6)}$$

Here R_e is the equilibrium radius defined by the condition that $R = R_e$ when $P = p_\infty$. The amplitude and the minimum pressure are related by the simple equation

$$A = (P_m/p_\infty)^{-1/3\gamma}. \quad \text{(B7)}$$

Then for a given A, p_∞, and γ, the corresponding P_m can be found from eq. (B7), and for this minimum pressure eq. (B1) solved. Thus the minimum radius R_m, the compression time T_c, and the second maximum radius R_{M2} are obtained. (Note that in case of constant ambient pressure p_∞ there is no sense in prolonging the integration of eq. (B1) beyond R_{M2}.)

During the bubble oscillation a pressure wave is radiated. The peak pressure in the wave, p_p, can be found using the $1/r$ law for diverging spherical waves as

$$p_p = P_p R_m/r. \quad \text{(B8)}$$

Here r is the point in the liquid where p_p is to be determined. The peak pressure at the bubble wall, P_p, and the maximum pressure at the wall, P_M, are related by eq. (3), and the pressure P_M can be found from eq. (B4) when substituting $R = R_m$.

To characterize the dissipation of energy by the oscillating bubble during the wall motion between two consecutive maximum radii, a damping factor, α, can be defined as

$$\alpha_i = R_{Mi+1}/R_{Mi}. \quad \text{(B9)}$$

It is convenient to display the quantities R_m, T_c and p_p in a non-dimensional form, using the relations:

$$Z_m = R_m/R_M, \quad T_{zc} = T_c/[R_M(\varrho_\infty/p_\infty)^{1/2}],$$
$$p_{zp} = (p_p/p_\infty) r/R_M.$$

Computations were performed for water under ordinary laboratory conditions, and an air bubble, i.e., the physical constants had the values:

$$p_{\infty i} = 100\ \text{kPa}, \quad \varrho_\infty = 1000\ \text{kg/m}^3, \quad c_\infty = 1450\ \text{m/s},$$
$$B = 300\ \text{MPa}, \quad n = 7, \quad \gamma = 1.4.$$

The scaling functions $Z_m(A)$, $\alpha(A)$, $T_{zc}(A)$, and $p_{zp}(A)$ thus obtained are displayed in Figs. 4 to 6.

References

[1] Leighton, T. G., Walton, A. J., An experimental study of the sound emitted from gas bubbles in a liquid. Eur. J. Phys. **8** [1987], 98–104.

[2] Pumphrey, H. C., Crum, L. A., Free oscillations of near-surface bubbles as a source of the underwater noise of rain. J. Acoust. Soc. Amer. **87** [1990], 142–148.

[3] Leighton, T. G., Wilkinson, M., Walton, A. J., Field, J. E., Studies of non-linear bubble oscillations in a simulated acoustic field. Eur. J. Phys. **11** [1990], 352–358.

[4] Samek, L., A multiscale analysis of nonlinear oscillations of gas bubbles in liquids. J. Acoust. Soc. Amer. **81** [1987], 632–637.

[5] Aymé-Bellegarda, E. J., Collapse and rebound of a gas-filled spherical bubble immersed in a diagnostic ultrasonic field. J. Acoust. Soc. Amer. **88** [1990], 1054–1060.

[6] Church, Ch. C., A theoretical study of cavitation generated by an extracorporeal shock wave lithotripter. J. Acoust. Soc. Amer. **86** [1989], 215–227.

[7] Vokurka, K., Beylich, A. E., Kleine, H., Experimental study of gas bubble oscillations using a shock tube. Acustica **75** [1992], 268–275.

[8] Bazhenov, V. Yu., Vasnetsov, M. V., Soskin, M. S., Taranenko, V. B., Dynamics of laser-induced bubble and free-surface oscillations in an absorbing liquid. Appl. Phys. B **49** [1989], 485–489.

[9] Ward, B., Emmony, D. C., Interactions of laser-induced cavitation bubbles with a rigid boundary. Proc. SPIE **1358** [1990], 1035–1045.

[10] Ward, B., Emmony, D. C., Interferometric studies of the pressures developed in a liquid during infrared-laser-induced cavitation-bubble oscillation. Infrared Physics **32** [1991], 489–515.

[11] Oliveri, S., Kattan, R., Denat, A., Numerical study of single-vapor-bubble dynamics in insulating liquids initiated by electrical current pulses. J. Appl. Phys. **71** [1992], 108–112.

[12] Smereka, P., Banerjee, S., The dynamics of periodically driven bubble clouds. Phys. Fluids **31** [1988], 3519–3531.

[13] Lu, N. Q., Prosperetti, A., Yoon, S. W., Underwater noise emissions from bubble clouds. IEEE J. Oceanic Eng. **15** [1990], 275–285.

[14] Carey, W. M., Low-frequency ocean surface noise sources. J. Acoust. Soc. Amer. Suppl. 1, **78** [1985], S1–S2.

[15] Carey, W. M., Low-frequency noise and bubble plume oscillations. J. Acoust. Soc. Amer. Suppl. 1, **82** [1987], S62.

[16] Crowther, P. A., Bubble noise creation mechanisms. Proc. NATO Adv. Workshop on Natural Mechanisms of Surface Generated Noise in the Ocean, Erice, Italy, 15–19 June 1987. In: Sea Surface Sound, Kerman, B. R., (Ed.), pp. 131–150. Reidel, Kluwer Academic Publishers, 1988.

[17] Hollett, R., Heitmeyer, R., Noise generation by bubbles formed in breaking waves. Proc. NATO Adv. Workshop on Natural Mechanisms of Surface Generated Noise in the Ocean, Erice, Italy, 15–19 June 1987. In: Sea Surface Sound, Kerman, B. R. (Ed.), pp. 449–462. Reidel, Kluwer, Academic Publishers, 1988.

[18] Pumphrey, H. C., Ffowcs Williams, J. E., Bubbles as sources of ambient noise. IEEE J. Oceanic Eng. **15** [1990], 268–274.

[19] Prosperetti, A., The thermal behaviour of oscillating gas bubbles. J. Fluid Mech. **222** [1991], 587–616.

[20] Longuet-Higgins, M. S., Resonance in nonlinear bubble oscillations. J. Fluid Mech. **224** [1991], 531–549.
[21] Longuet-Higgins, M. S., Nonlinear damping of bubble oscillations by resonant interaction. J. Acoust. Soc. Amer. **91** [1992], 1414–1422.
[22] Vokurka, K., Excitation of gas bubbles for free oscillations. J. Sound Vib. **106** [1986], 275–288.
[23] Smulders, P. T., van Leeuwen, H. J. W., Experimental results on the behaviour of a translating gas bubble in water due to a pressure step. In: Finite-Amplitude Wave Effects in Fluids, Bjørnø L. (Ed.). IPC Science and Technology Press, Guildford 1974, pp. 227–233.
[24] Jensen, F. B., Shock-excited pulsations of large air bubbles in water. Trans. ASME, J. Fluids Eng. **96** [1974], 389–393.
[25] Shima, A., Tomita, Y., Takahashi, K., The collapse of a gas bubble near a solid wall by a shock wave and the induced impulsive pressure. Proc. Inst. Mech. Eng. **198C** [1984], 81–86.
[26] Vokurka, K., Amplitudes of free bubble oscillations in liquids. J. Sound Vib. **141** [1990], 259–275.
[27] Vokurka, K., Free oscillations of a cavitation bubble. J. Sound Vib. **135** [1989], 399–410.
[28] Cole, R. H., Underwater Explosions. Princeton University Press, Princeton 1948.
[29] Tomita, Y., Shima, A., Ohno, T., Collapse of multiple gas bubbles by a shock wave and induced impulsive pressure. J. Appl. Phys. **56** [1984], 125–131.
[30] Vokurka, K., Comparison of Rayleigh's, Herring's, and Gilmore's models of gas bubbles. Acustica **59** [1986], 214–219.